5. De Vis K, Schelstraete K, Deman J, Vermeulen FL, Sambre J, Goethals P, Van Haver D, Slegers G, Vandecasteele C, De Schryver A. Clinical comparison of ^{11}C-ACPC (α-amino cyclopentane carboxylic acid) and ^{13}N-ammonia as tumor tracer. *Acta Oncol* 1987;26:105–111.
6. Strauss LG, Conti PS. The applications of PET in clinical oncology. *J Nucl Med* 1991;32:623–647.
7. Silvestrini R, Daidone MG, Valagussa P, Di Fronzo G, Mezzanotte G, Mariani L, Bonadonna G. ^{3}H-Thymidine-labeling index as prognostic indicator in node-positive breast cancer. *J Clin Oncol* 1990;8:1321–1326.
8. De Reuck J, Sieben G, De Coster W, Roels H, vander Eecken H. Cytophotometric DNA determination in human oligodendoglial tumors. *Histopathology* 1990;4:225–232.
9. Martiat Ph, Ferrant A, Labar D, Cogneau M, Bol A, Michel C, Michaux JL, Sokal G. In vivo measurement of carbon-11-thymidine uptake in non-Hodgkin's lymphomas using PET. *J Nucl Med* 1988;29:1633–1637.
10. van Eijkeren ME, De Schryver A, Goethals P, Poupeye E, Schelstrate K, Lemahieu I, De Potter C. Measurement of short-term ^{11}C-thymidine uptake in tumors of the head and neck using positron emission tomography. *Acta Oncol* 1992;31:539–543.
11. Shaw T, Mac Phee DG. Rapid and complete degradation of thymidine by human peripheral blood platelets: implications for genotoxicity assays. *Mut Res* 1986;163:75–80.
12. Vander Borght T, De Maeght S, Labar D, Goethals P, Pauwels S, van Eijkeren M. Comparison of thymidine labeled in methyl group and in 2C-position in human PET studies [Abstract]. *Eur J Nucl Med* 1992;19:578.
13. Thierens H, van Eijkeren M, Goethals P. Biokinetics and dosimetry for [methyl-^{11}C]thymidine. *Br J Radiol* 1994;67:292–295.

Enhancement of Radiation Dose to the Nucleus by Vesicular Internalization of Iodine-125-Labeled A33 Monoclonal Antibody

Farhad Daghighian, Els Barendswaard, Sydney Welt, John Humm, Andrew Scott, Mark C. Willingham, Eileen McGuffie, Lloyd J. Old and Steven M. Larson

Departments of Medical Physics, Ludwig Institute for Cancer Research, Immunology Service, Laboratory of Nuclear Medicine Research, Memorial Sloan-Kettering Cancer Center, New York, New York; and Department of Pathology and Laboratory Medicine, Medical University of South Carolina, Charleston, South Carolina

In radioimmunotherapy, the emission characteristics of the radioisotope is critical in determining the radiation dose to the tumor compared to normal organs. If antibodies internalize and transport low-energy electron emitting isotopes close to the tumor cell nucleus, an improved therapeutic advantage is achieved. **Methods:** Using fluorescent microscopy, we studied the subcellular distribution of an internalizing antibody, A33, which detects a restricted determinant on colon cancer cells. We developed a physical model to assess the dose deposited in the nucleus by electrons emitted from radiolabeled A33 accumulated inside vesicles. This model is based on the energy-range relationship of electrons in water. Similarly, another model was developed to calculate the radiation dose to the nucleus from electrons emitted from extracellular space. The percentage of A33 bound to membrane and internalized was determined in vitro at various time points. Cytotoxicity experiments were performed with ^{125}I- and ^{131}I-labeled A33 at various concentrations and specific activities. **Results:** A33 accumulates in cytoplasmic vesicles (40% of total bound) which transport the activity close to the nucleus. This increases the radiation dose to the cancer cell nucleus by a factor of 3 compared to the average dose calculated based on the assumption of a uniform distribution on the cell membrane. The cytoplasm of antigen-negative normal cells shields the nucleus from the electrons emitted from extracellular ^{125}I. This shielding is 30 times less for ^{131}I. Cytotoxicity data show 10% cell survival with 10 μCi/ml of ^{125}I-A33, but 90% survival with up to 100 μCi/ml of ^{125}I-A33 in the presence of a blocking dose of 100-fold excess of cold A33. Similar experiments with ^{131}I showed cytotoxicity in both cases. **Conclusions:** The results of the cytotoxicity experiment are in agreement with the physical model and suggest a basis for improved tumor-to-marrow radiation dose by clinical use of ^{125}I-A33.

Key Words: Auger electrons, cell-level dosimetry; monoclonal antibody; vesicular internalization

J Nucl Med 1996; 37:1052–1057

Isotope selection strategies for the radioimmunotherapy (RIT) of cancer have been greatly influenced by the general observation that antigen expression in tumors is heterogeneous. In addition, attention has been focused on the apparent poor penetrability of tumors by monoclonal antibodies (MAbs) (*1–4*). For these reasons, the majority of clinical studies have utilized long-range beta emitters (^{131}I, ^{90}Y), which irradiate cells up to 1 or 2 mm from the site of the radioisotope decay. As a consequence of the long-range electrons, the bone marrow receives a high radiation dose from radiolabeled MAb in the blood, limiting the amount of radioactivity which can be administered (*5–8*).

The A33 antigenic system was selected as a model for low-energy emitter RIT because it shows high uniform expression on colon cancer-tissue sections by immunohistochemical techniques. Binding studies on colon cancer cell lines demonstrate relatively high expression (800,000 MAb A33 molecules bound per cell), and radiolabeled MAb A33 is internalized into cells (*9*). In clinical studies, autoradiographs of biopsied colon cancer metastases show relatively uniform distribution of the intravenously administered radiolabeled antibody within these tumors with excellent tumor to normal tissue ratio (*10*).

The prevalent electron emissions from ^{125}I are Auger electrons ranging in energy from a few electron volts to 28 keV (*11*). In addition, there is a small yield (7%) of internal conversion electrons at 32 keV. Photon emissions do not locally deposit their energy and therefore can be neglected in dose calculations to individual cells. Their contribution, however, will not be negligible in patient studies. The radiotoxicity of ^{125}I, when directly incorporated into DNA, is quite high; as few as 100 decays will kill a cell (e.g., ^{125}I-labeled IUDR) (*12–14*). This radiotoxicity is attributed to the prolific emission of very short-range electrons (<20 nm) which acts as high LET radiation (*12*). The radiotherapeutic effects of Auger-emitting isotopes has been studied both experimentally and theoretically (*15,16*).

It is widely believed that the cell nucleus, and more specif-

Received May 8, 1995; revision accepted Nov. 20, 1995.
For correspondence or reprints contact: Farhad Daghighian, PhD, Department of Medical Physics, Memorial Sloan-Kettering Cancer Center, 1275 York Ave., New York, NY 10021.

ically the nuclear DNA, is the most radiosensitive part of the cell and the critical target for cytotoxic radiotherapy (*12*). The radiation dose from electrons and alpha emissions of several radioisotopes were calculated by Goddu et al. (*17*) for a variety of cell and nuclear diameters. They considered the radioactivity to be uniformly distributed in a source region and calculated the absorbed dose fractions. The source regions considered were the nucleus, cytoplasm and cell surface. The target regions were the nucleus and the cell.

In this article, we demonstrate that MAb A33 internalizes into the target cells via large cytoplasmic vesicles. We present a physical model to calculate the radiation dose to the nucleus from the ^{125}I-labeled A33 entrapped in these vesicles. We also show that ^{125}I-A33 can be specifically cytotoxic to antigen-positive target cells in vitro, and the observed cytotoxic doses are predicted by the model.

MATERIALS AND METHODS

Cell Lines

The human colon carcinoma cell line SW1222 was obtained from Sloan-Kettering Institute's cell bank. Cells were cultured in Eagle's minimum essential medium (MEM), containing 2 m*M* glutamine, 1% nonessential amino acids, 100 U/ml penicillin and 100 μg/ml streptomycin (MEM) and supplemented with 10% fetal bovine serum (FBS). Cultures were frequently tested for mycoplasma.

Monoclonal Antibodies

Characterization and labeling procedures: MAb A33 (IgG_{2a}) and control MAb FB5 (IgG_{2a}) were purified from high-titered, centrifuged and filtered ascites fluid on protein A-Sepharose (Pharmacia) using 0.05 *M* Tris HCl/0.15 N NaCl, pH 8.6, as starting buffer and 0.05 *M* sodium acetate/0.15 N NaCl, ph 4.0, as eluting buffer. The eluted fractions were pooled and passed over a Sephadex G-25 column in phosphate-buffered saline, pH 7.0. Iodination was carried out with the chloramine-T method using 10.0 mCi (cytotoxicity studies) or 1.0 mCi (binding studies) ^{125}I or 1 mCi ^{131}I per 100 μg antibody and 10 μg of chloramine-T at 1.0 mg/ml. PBS containing 0.05% bovine serum albumin and 10 m*M* NaI was used as the buffer for subsequent size-exclusion chromatography with Sephadex G-25 chromatography. Immunoreactivity was measured by a cell absorption assay as previously described (*9,18*) and ranged from 50% to 70%.

Binding and Internalization Studies

SW1222 colon cancer cells were plated into 24 well plates at 250,000 cells per well. After 24-hr incubation at 37°C, 1 μg/ml of ^{125}I-A33 was added. At various time points, the radioactive counts per minute (CPM) were measured in a well counter in quadruplicate to determine the total radioactivity that was cell-associated, cell-surface bound and internalized. Total CPM bound was defined as the CPM remaining after the adherent target cells were washed with PBS × 2 and cells lysed with 0.02% s.d.s. The cell-surface-bound CPM was determined by exposure of washed cells to 0.05 *M* of glycine, 0. 15 N NaCl pH 2.6 buffer. CPM removed in acid buffer were considered cell-surface-bound. Similar results were obtained with glycine buffer containing high salt (3.0 N NaCl). After the cell surface fraction of bound antibody was removed, the internalized fraction was determined by measuring remaining CPM by SDS lysis. For each measurement of CPM bound, the net CPM bound was determined by subtraction of the background (wells pretreated with excess unlabeled MAb A33) from the positive (wells blocked with control IgG_{2a} MAb).

SW1222 cells were plated in 35 mm tissue culture dishes and incubated (at 37°C) with MAb A33 or an isotype-matched control IgG_{2a} (MAb FB-5 IgG_{2a}) at 1 μg/ml. After 6 hr cells were washed, exposed to an acid wash solution and then fixed with 3.7% formaldehyde and subsequently incubated in the presence of 0.1% saponin with rhodamine-labeled goat anti-mouse IgG to detect internalized MAb A33. Cells were examined under phase contrast and fluorescence microscopy (*19*). The cell-surface component of bound MAb A33 was removed by acid wash to facilitate visualization of the internalized component.

In Vitro Cytotoxicity Studies

SW1222 cells were plated at 500,000 cells/well into six well plates and incubated for 24 hr 37°C to allow for cell adherence. Iodine-125-A33 was then added at concentrations from 1 μCi/ml to 100 μCi/ml (0.01 to 1 μg/ml), total of 2 ml/well (in presence of excess isotype-matched control MAb FB-5 IgG_{2a}). Two sets of control experiments were conducted: (1) wells containing only 100 μg/ml of non-radioactive MAb A33 (no radioactivity, cell growth control); and (2) control wells containing varying radioactive doses of ^{125}I-A33 pretreated with 100 times excess unlabeled MAb A33 (100.0 μg/ml) to block cell-surface binding of radiolabeled antibody (and to control for radiation dose delivered from supernatant).

To evaluate cell kill, cell counts on day 9 were done by removing surviving cells with trypsin/EDTA and after washing three times. Viable cells were counted under phase contrast microscopy using a hemocytometer. The percent cell survival was scored as number of viable cells/500,000 cells × 100. To evaluate inhibition of cell growth, percent inhibition was defined as the number of viable cells in wells treated with ^{125}I-A33 and blocked by excess MAb A33 per viable cells in wells treated with non-radioactive MAb A33. The same experiments were done with ^{131}I-labeled MAb A33.

RESULTS

Binding and Internalization Studies

A fluorescence micrograph of a cluster of SW1222 cells (Fig. 1) demonstrates MAb A33 concentrated in vesicles (macropinosomes). In this example, several of the vesicle containing MAb A33 are in close proximity to the cell nucleus. Approximately 40%–50% of the ^{125}I-A33 MAb added to the wells was bound to SW1222 colon carcinoma cells after 24 hr, and 35%–40% of the total bound CPM was internalized (resistant to removal with acid wash) (Fig. 2).

In Vitro Cytotoxicity Studies

In the positive wells, unblocked ^{125}I-A33 was cytotoxic (>90% cell kill) at the 10–15 μCi/ml dose range. While other cell structures, such as the membranes of the vesicles, received significantly higher radiation doses the morphologic appearance of the ^{125}I-A33-treated cells suggests that the critical damage is to the nucleus. The cells developed bizarre, large, multinucleated forms similar to those observed with external gamma irradiation and then underwent autolysis.

The cytotoxic effect decreased to less than 10% cell kill at the 2.5 to 5 μCi/ml ^{125}I-A33 dose range, although a cell growth inhibitory effect was still present. In addition to the cytotoxic effects, microscopic examination of these wells on days 4 to 5 revealed that morphologic changes were evident in the positive wells and the treated cells transformed into multi-nucleated giant cells prior to cell death (Fig. 3). In the first control experiment, cells grown in the presence of unlabeled MAb A33 had the same doubling times as the untreated cells (data not shown), demonstrating that MAb A33 had no effect on cell growth by itself. In the second control experiment, control wells containing varying radioactive doses of ^{125}I-A33 were pretreated with 100 times excess unlabeled MAb A33 (100.0 μg/ml) to block cell-surface binding of radiolabeled antibody. The percent inhibition on day 4 showed that the presence of ^{125}I-A33 in the supernatant inhibited cell growth by 50% (doses of 60 to 100 μCi/ml), and little cell death was observed (<10%)

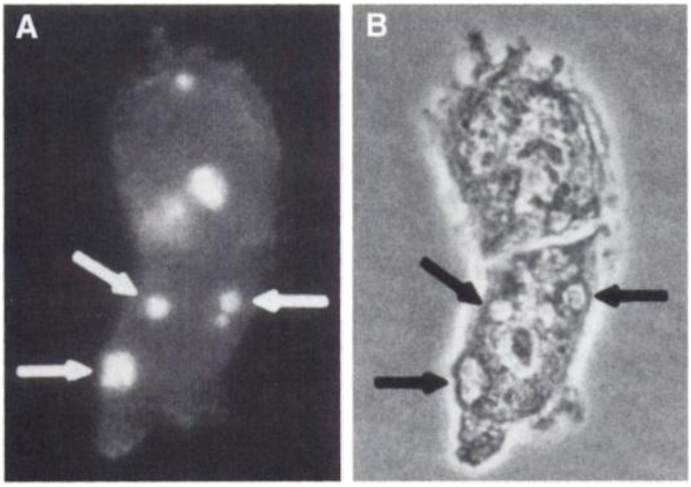

FIGURE 1. A fluorescent photomicrograph of SW1222 colon carcinoma cells (A) and a phase contrast photomicrograph (B) of the same cells depicting the internalized fraction of MAb A33 detected using a fluoresceinated second anti-mouse reagent. MAb A33 concentration in the cytoplasmic vesicles (macropinosomes) is shown.

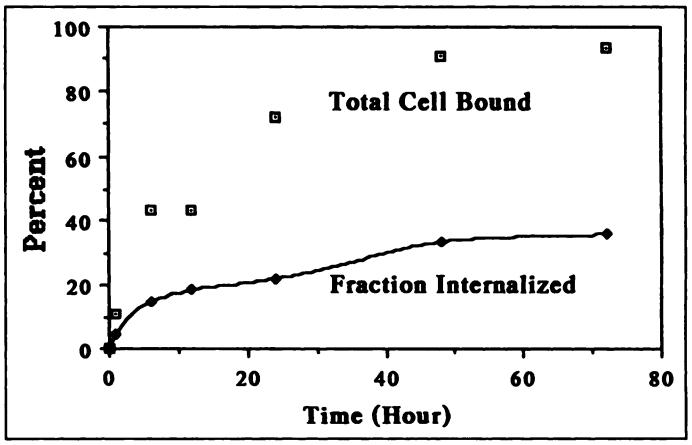

FIGURE 2. Distribution of cell-bound ^{125}I-A33: (a) total cell-bound radioactivity and (b) fraction of radioactivity internalized into the cell (acid-resistant).

(Fig. 2). These studies demonstrate that cell binding was necessary for the cytotoxic effect.

In contrast, identical experiments with ^{131}I-A33 showed cytotoxicity in wells to which excess unlabeled MAb A33 was added, indicating that the long-range electron emission from supernatant ^{131}I-A33 deposited significant amount of radiation dose into the cell nucleus (cross-fire effect).

Cell Level Radiation Dose Calculations

The energy absorbed in the nucleus per disintegration of ^{125}I and ^{131}I contained within a vesicle is plotted with respect to the gap between the vesicle and the nucleus (i.e., $L - R_n - R_v$) (Fig. 1). The sharp decrease in radiation dose to the cell nucleus was mainly due to the decreasing probability of electrons crossing the nucleus (the solid-angle effect). The energy deposited in the nucleus was higher for ^{125}I than for ^{131}I when the gap was less than 0.2 μ (due to high yield of electrons with energies of 3 keV) but they became almost equal at larger distances. Figure 4 also shows that the absorbed energy increased with cell nucleus size, but that energy per unit mass (absorbed dose) decreased.

Table 1 shows the S-values for the nucleus from the vesicles containing ^{125}I or ^{131}I for several cell dimensions. In addition, the S-values from the radioactivity on the membrane, uniformly distributed in cytoplasm, and the nucleus are presented as calculated by Goddu et al. (*17*). For cells with Rn = 2 and Rc = 5 μ, the vesicular radiation dose to the nucleus per disintegration was five times greater than the radiation dose per disintegration from the cell membrane. This ratio decreased for larger nuclei and was lower for ^{131}I. On average, the dose to the nucleus from decays within vesicles was three times greater than for decays on the cell membrane for ^{125}I and about twice greater for ^{131}I.

Dose from MAb Outside the Cell

The energy per disintegration per milliliter of extracellular fluid was calculated for ^{125}I and ^{131}I for various cell dimensions. The radiation dose for ^{125}I was 1.2×10^{-12} Gy/Bq · s per ml of extra-cellular fluid, and 3.7×10^{-11} Gy/Bq · s per milliliter of extra-cellular fluid for ^{131}I. Only a small dependence on the cell dimensions was observed. A much greater difference between ^{125}I and ^{131}I was seen when the dose to the cell nucleus from radioactivity in the extra-cellular fluid was calculated. This is because the dose contribution to the cell nucleus from ^{125}I decays results principally from Auger electrons within a 20 μ range of the cell, whereas in the case of ^{131}I the volume integral extends to the full range of the electron emissions.

Application of the Model to the Cytotoxicity Studies

Using the average values (Table 1; last row), we calculated the dose to nucleus from membrane-bound and internalized MAb (Table 2). In the ^{125}I-A33 unblocked cytotoxicity experiment (positive wells), the <10% cell survival was seen at a concentration between 10 to 15 μCi/ml. In the calculation, the average value of 12.5 μCi/ml was used. In the second control experiment, in which ^{125}I-A33 was blocked by excess MAb A33, 90% cell survival was observed at concentrations between

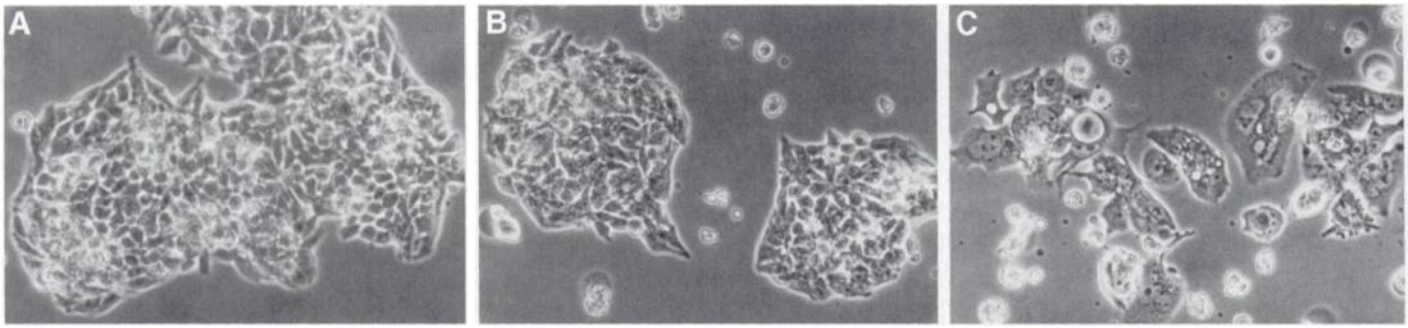

FIGURE 3. Photomicrograph demonstrating morphologic effects of ^{125}I-A33 on SW1222 human colon carcinoma cells that were exposed to radiolabeled MAb A33 continuously for 4 days. (A) control SW1222 cells cultured in the presence of nonradioactive MAb A33. (B) control SW1222 cells cultured in the presence of ^{125}I-A33 with excess unlabeled MAb A33 added to block antibody binding to cell membrane A33 antigen. Reduced cell number is apparent although morphologically cells are similar to those in top panel. (C) SW1222 cells exposed to ^{125}I-A33 (unblocked), shows SW1222 cells at same magnification as above. Marked morphologic changes are apparent in the cell prior to cell death.

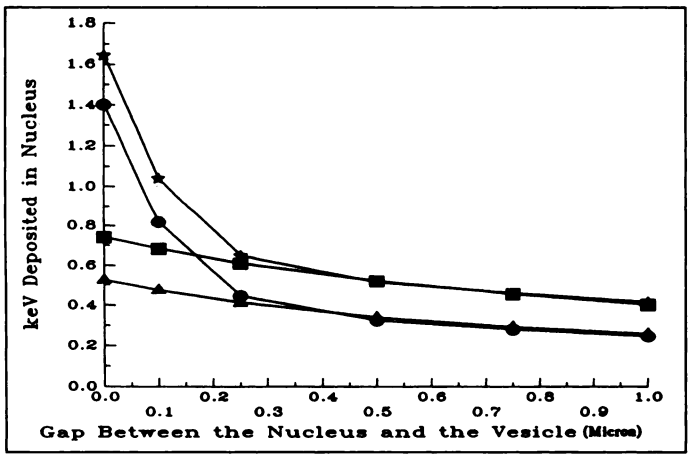

FIGURE 4. The energy deposited in the cell nucleus by the electrons of ^{125}I and ^{131}I. The source of emission is a vesicle of 0.5 μ diameter located at various distances from the nucleus. Two different nuclear radii were considered: 3 μ (triangle for ^{131}I and circle for ^{125}I), and 4 μ (rectangle for ^{131}I and star for ^{131}I).

60 to 100 μCi/ml. For our calculation, the average value of 80 μCi/ml was considered. In these experiments, the total number of cells increased from 500,000 to 3 million by day 4. Although the cell numbers decreased after day 4 in the unblocked ^{125}I-A33 wells, we assumed the maximum number of cells (3 million) (see Eq. A8) since the radioactivity in the viable cells would not increase due to the loss of other cells. The fractions of MAb on the membrane and in the vesicles (f_m and f_v in Eq. A8) were estimated from Figure 2. Table 2 also shows the radiation doses that resulted from a uniform solution of ^{125}I in the extracellular space (free).

DISCUSSION

The potency of Auger electrons in delivering radiation damage when incorporated into DNA is well documented (*12–15*). Iodine-125-IUdR incorporated into DNA is the major model of this therapeutic approach; however, its clinical application is limited by lack of specific tumor targeting and cell-cycle dependency (*20–23*). In general, radiation damage from electrons of ^{125}I can be subdivided into two categories: (1) when ^{125}I is incorporated into DNA, the prolific emission of very low-energy electrons results in significant local, high-LET-type damage, leading to an average of one DNA double-strand break per decay; and (2) when ^{125}I decay occurs farther than 10 nm from the DNA, the damage results from longer-range electron emissions, is low-LET in nature, and is therefore less effective.

Fluorescence microscopy studies presented in this article (Fig. 1) show that MAb A33 internalizes into the target cells via macropinosomes, large cytoplasmic vesicles which traverse the cytoplasm and come into close proximity to the nucleus. It can be postulated that the majority of MAbs that internalize do so via cytoplasmic vesicles (*19*), and a substantial contribution of the dose to the nucleus arises from radioisotopes entrapped within vesicles. This contribution has not been previously considered. In this paper, we present a physical model to estimate radiation dose to the nucleus from electrons emitted from cytoplasmic vesicles, based on the energy-range relationship for electrons (*24*).

These calculations demonstrate that the transport of ^{125}I to within 1–2 μ from the cell nucleus results in the deposition of energy from the internal conversion electrons as well as the K and L Auger electron series. This proximity results in a significant enhancement of the radiation dose to the nucleus when compared to the assumption of only membrane-bound radioactivity. Also presented in this paper is a physical model for calculation of the absorbed dose to the nucleus from electrons which are emitted from outside the cell. This model demonstrates that the cytoplasm shields the nucleus from absorbing energy from ^{125}I electrons emitted outside the cell, but has minimal stopping power for higher energy electrons such as those of ^{131}I. For such internalizing MAbs, radiolabeling with ^{125}I would have a significant dosimetric advantage over ^{131}I with regard to anti-tumor effects versus normal organ toxicity (particularly bone marrow).

Studies of ^{125}I targeting to the cell membrane using MAbs have shown that greater than 100,000 decays are required for one log of cell kill (*25,26*). Yet, MAbs capable of internalizing isotope into various cytoplasmic compartments may offer a substantial enhancement in dose to antigen-positive cells with no concomitant increase in dose to antigen-negative cells of normal tissues. This study demonstrates the feasibility of estimating the radiation gain achieved by such MAb systems. We also show that ^{125}I-A33 can be specifically cytotoxic to antigen-positive target cells in vitro, in agreement with our model. Measurements over time of the level of MAb A33-directed isotope internalization and retention in cytoplasmic vesicles show that a 3-fold increase in radiation dose can be delivered to the cell nucleus, as a result of this MAb's internalization characteristics. Preliminary in vivo studies have demonstrated that ^{125}I-A33 also causes regression of established human colon cancers growing in nu/nu mice at non-toxic serum levels (*9*). These results are consistent with model predictions that the nuclei of antigen-negative cells (e.g., bone marrow cells) will be protected from extracellular, low-energy electrons due to shielding by their cytoplasm.

While the model uses an idealized spherical cell with a centrally placed nucleus, a significant fraction of colon carci-

TABLE 1
S-Values (in cGy/Bq · s) of Radiation to the Nucleus from Iodine-125 or Iodine-131

Rn	Rc	^{125}I Membrane to Nucl.	^{125}I Vesicle to Nucl.	^{125}I Cytoplasm to Nucl.	^{125}I Nucleus to Nucl.	^{131}I Membrane to Nucl.	^{131}I Vesicle to Nucl.	^{131}I Cytoplasm to Nucl.	^{131}I Nucl. to Nucl.
2	5	0.023	0.100	0.071	4.79	0.026	0.063	0.054	0.498
3	5	0.024	0.063	0.060	1.50	0.027	0.046	0.045	0.199
4	5	0.026	0.056	0.059	0.66	0.028	0.037	0.039	0.106
3	6	0.0175	0.048	0.041	1.5	0.017	0.037	0.034	0.199
4	6	0.018	0.038	0.037	0.66	0.018	0.029	0.029	0.106
Average		0.021	0.061	0.054	1.822	0.023	0.042	0.040	0.221

*Constrained within a vesicle with 0.25 μ radius averaged over various distances from the nucleus. The S-values from the radioactivity localized on the membrane, uniformly distributed in the cytoplasm and from within the nucleus of the cell are also presented (see Appendix).

TABLE 2
Absorbed Radiation Dose (in cGy) for Cytotoxicity Experiment

Tracer	Membrane	Vesicle Bound	Free	Total	Observed Cell Viability
^{125}I-A33 (12.5 μCi/ml with 0.1 mg/ml control MAb)	3429	3795	40	7265	<10%
^{125}I-A33 (3.75 μCi/ml with 0.1 mg/ml control MAb)	1029	1128	12	2170	90%
^{125}I-A33 (80 μCi/ml with 0.1 mg/ml nonradioactive MAb A33)	219	243	276	744	>90%

*Experiment had (a) 12.5 μCi/ml of ^{125}I-A33 added to 500,000 cells for 9 days (specific activity of 100 μCi/μg), and (b) excess unlabeled A33 was added to 80 μCi/ml of ^{125}I-A33 (final specific activity of 1 μCi/μg), where it is assumed that due to binding of non-radioactive A33 the amount of radioactivity bound to the cells is 6.5% of the first case.

noma cells in culture or in tissues deviates from this idealized form. In some cases, cells have eccentric nuclei so that even cell membrane-bound antibody may be close enough to the nucleus to contribute to the dose.

As the exact distance of the vesicle to nucleus was not known, we assumed the vesicles to be distributed evenly throughout the cytoplasm. Therefore, the absorbed dose from the vesicular radiation was almost the same as that from uniformly distributed radioactivity from the cytoplasm (see Table 1). Our model is, however, closer to the physiologic nature of vesicular MAb internalization, since internalizing antibodies have in general been observed to accumulate in distinct subsets of vesicles, and the distribution of these vesicles in the cytoplasm may be unique for each type of vesicle or antigenic system. Although some vesicular structures, such as caveolae, remain in close proximity to the cell membrane, they would be unlikely to support Auger irradiation of the nucleus. For a substantial gain to occur, the MAb must internalize sufficient ^{125}I in a region of the cytoplasm close to the nucleus for a sufficient length of time. It is difficult to develop an accurate dose-response relationship for studies involving short-range electron-emitting isotopes, due to strong dosimetric dependence upon source distribution. In the future, we propose to refine our knowledge of the ^{125}I distribution by combining information from various microscopic imaging techniques to study and quantitate this distribution. If only a small fraction of metabolic products of A33 containing the ^{125}I radionuclide diffuse into the cell nucleus, the radiation dose will be enhanced significantly. Table 1 shows that the S-value for nucleus-to-nucleus radiation of ^{125}I Auger electrons is 90 times larger than that of vesicle-to-nucleus radiation. Therefore, even if radioactivity in the nucleus is only 1% of that on the membrane, the total dose would be 40% higher. This analysis demonstrates the importance of investigating the fate of MAbs and isotope after cell-binding. Strategies to transport ^{125}I into the nucleus, and ways to measure it, need to be explored.

These results emphasize the importance of evaluating the cellular internalization and transport characteristics of each antigen-antibody system and of developing cell-level dosimetry methods. There is a selective advantage (tumor/bone marrow) of low-energy emitting isotopes (e.g., ^{125}I) vis-a-vis long-range electron-emitting isotopes (e.g., ^{131}I) currently employed in RIT trials when tumor expression of the antigen is uniform (as in the A33 MAb system).

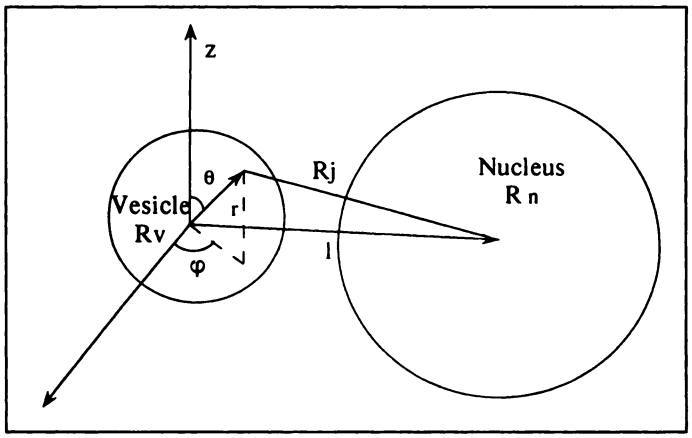

FIGURE A1. The radiolabeled antibody is accumulated in the vesicle at a distance L from the nucleus.

APPENDIX

Physical Model for Dose Calculation

Consider an electron with initial energy e_j. As it travels through the cell medium, it constantly loses energy to its final range $R(e_j)$. The energy E (eV) and range (nm) of an electron in unit density matter are related by (*27*):

$$E(R) = 119.1(R + 7)^{0.565} + 4.23 \times 10^{-4} R^{1.33} - 367. \quad \text{Eq. A1}$$

The energy deposited in a small distance dr between r and r_+dr is:

$$dE = dr \times [dE/dR]|_{R(e_j)-r}. \quad \text{Eq. A2}$$

The energy deposited in the nucleus from an electron with initial energy e_j emitted at a distance R_j from the center of the nucleus is given by:

$$\varepsilon_n(R_j; e_j) = \int [dE/dR]|_{R(e_j)-r}[0.5 - (r^2 + R_j^2 - R_N^2)/4rR_j]\, dr, \quad \text{Eq. A3}$$

where the limits of integration are from $R_j - R_N$ to either $R_j + R_N$ or $R(e_j)$ if the particle stops in the nucleus.

Dose from the MAb Concentration in a Vesicle

The nucleus and vesicles are assumed to be spheres with radii R_n and R_v, respectively (Fig. A1), with a distance L between their centers. R_j is calculated in terms of the position of the isotope disintegration (r, θ, φ):

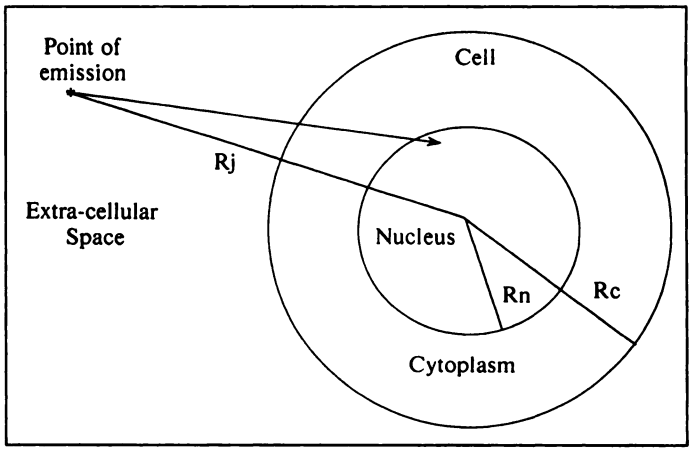

FIGURE A2. A case in which the radiolabeled antibody is not bound to the cell and is located in the extra-cellular space. The cytoplasm shields the cell nucleus from low-energy electrons.

$$R_j = (r^2 + L^2 - 2rL \sin\theta \sin\varphi)^{0.5}. \quad \text{Eq. A4}$$

The energy per disintegration deposited to the nucleus from the electrons is:

$$E_n = (1/(4/3\pi R_v^3)) \sum_j P_j \times \int_0^{2\pi} \int_0^{\pi} \int_0^{Rv} \varepsilon_n(R_j; e_j) r^2 \sin\theta \, dr \, d\theta \, d\varphi. \quad \text{Eq. A5}$$

Dose from MAb in Extra-Cellular Space. Assuming a cell with radius Rc, and an electron with energy e_j emitted from outside the cell at distance R_j (>Rc) (Fig. A2), the energy deposited to the nucleus per disintegration per ml of extracellular fluid is:

$$E_{ECS} = (1/(1\ \text{ml})) \sum_j P_j \times 4\pi \int_{Rc}^{R(e_j)} \varepsilon_n(R_j; e_j) R_j^2 dR_j. \quad \text{Eq. A6}$$

Calculations of the S-Values. The mean absorbed radiation dose to the cell nucleus, D_{nucl}, is:

$$D_{nucl} = A_{source} \times S, \quad \text{Eq. A7}$$

where A_{source} is the cumulated activity in the source region. S is the radiation dose to the cell nucleus per disintegration. The unit for the S-value is Gy/Bq · s (1 keV/g = 1.602×10^{-13} Gy). In our calculations we assumed cells with a nuclear radii of 2, 3 and 4 μ; and vesicle radius of 0.25 μ. The cell radius varied between 5 to 7 μ, and it was assumed that each vesicle spends equal time at each distance between the cell membrane and the nucleus. Therefore the energies from different vesicular distances were averaged.

Calculating Dose to Cell in Cytotoxicity Studies

The dose to the nucleus from the vesicles and membrane in the cytotoxicity experiment is:

$$D_{nucl} = (\text{Radioactivity in the well}) \times \left\{ S_v \int dt\, f_v(t)/N(t) + S_m \int dt\, f_m(t)/N(t) \right\}, \quad \text{Eq. A8}$$

where $f_v(t)$ and $f_m(t)$ are the fractions of radioactivity in vesicles and membrane, respectively (see results of the binding experiment, Fig. 2); S_v and S_m are the S-values for vesicle-to-nucleus and membrane-to-nucleus, respectively. N(t) is the total number of cells.

The radiation dose deposited into the cell nucleus from the radioactive solution in the extracellular space was calculated by multiplying the supernatant radioactive concentration (in Bq/ml) by exposure time (in seconds) and then by the S-values (in Gy/Bq · s per ml) found using Equations A6 and A7.

ACKNOWLEDGMENTS

We thank Drs. G. Sgouros and M.C. Graham for many useful discussions. This work was supported in part by Department of Energy grant De FG02-86ER60407 and National Cancer Institute grants CA 08748 and CA033049.

REFERENCES

1. Jain RK, Baxter MJ. Mechanism of heterogeneous distribution of monoclonal antibodies and other macromolecules in tumors: significance of elevated interstitial fluid pressure. *Cancer Res* 1988;48:7022–7032.
2. Ong GL, Mattes MJ. Penetration and binding of antibodies in experimental human solid tumors grown in mice. *Cancer Res* 1989;49:4264–4273.
3. Juweid M, Neumann R, Paik C, et al. Micropharmacology of monoclonal antibodies in solid tumors: direct experimental evidence for a binding site barrier. *Cancer Res* 1992;52:5144–5153.
4. Jain RK. Vascular and interstitial barriers to delivery of therapeutic agents in tumors. *Cancer Metastasis Rev* 1990;9:253–266.
5. Humm JL. Dosimetric aspects of radiolabeled antibodies for tumor therapy. *J Nucl Med* 1986;27:1490–1497.
6. Mausner LF, Srivastava SC. Selection of radionuclides for radioimmunotherapy. *Med Phys* 1993;20:503–509.
7. Larson SM, Raubitschek A, Reynolds JC, et al. Comparison of bone marrow dosimetry and toxic effect of high dose ^{131}I-labeled monoclonal antibodies administered to man. *Int J Radiat Appl Instrum* 1989;16:153–158.
8. De Nardo GL, De Nardo SJ, Macey DJ, Shen S, Kroger LA. Overview of radiation myelotoxicity secondary to radioimmunotherapy using ^{131}I-Lym-1 as a model. *Cancer* 1994;73:1038–1048.
9. Barendswaard EC, Welt S, Divgi CR, Garin-Chesa P, Williams C, Old LJ. Anti-colon cancer monoclonal antibody 100-310: in vitro studies and in vivo localization [Abstract]. *Proc American Assoc for Cancer Res* 1992;33:345.
10. Welt S, Divgi CR, Real FX, et al. Quantitative analysis of antibody localization in human metastatic colon cancer: a phase I study of monoclonal antibody A33. *J Clin Oncol* 1990;8:1894–1906.
11. Howell RW. Radiation spectra for Auger-electron emitting radionuclides: report no. 2 of AAPM Nuclear Medicine Task Group No. 6. *Med Phys* 1992;19:1371–1383.
12. Kassis AI, Howell RW, Sastry KSR, Adelstein SJ. Positional effects of Auger decays in mammalian cells in culture. In: Baverstock KF, Charlton DE, eds. *DNA Damage by Auger Emitters.* London, Taylor and Francis;1988;1–14.
13. Hofer KG, Harris CR, Smith JM. Radiotoxicity of intracellular ^{67}Ga, ^{125}I, ^{3}H: nuclear versus cytoplasmic radiation effects in murine L1210 leukemia. *Int J Radiat Biol* 1975;28:225–241.
14. Hofer KG. Radiation biology and potential therapeutic applications of radionuclides. *Bull Cancer (Paris)* 1980;67:343–353.
15. Howell RW, Narra VR, Sastry KSR, Rao DV, eds. *Biological aspects of Auger processes.* American Institute of Physics, Woodbury, N.Y. 1992.
16. Humm JL, Howell RW, Rao DV. Dosimetry for Auger electron emitters: report No. 3 of AAPM Nuclear Medicine Task Group No. 6. *Med Phys* 1994;21:1901–1915.
17. Goddu SM, Rao DV, Howell RW. Multicellular dosimetry for micrometastases: dependence of self-dose versus cross-dose to cell nuclei on the type and energy of radiation and subcellular distribution of radionuclides. *J Nucl Med* 1994;35:521–530.
18. Welt S, Divgi CR, Kemeny N, et al. Phase I/II study of iodine-131: labeled monoclonal antibody A33 in patients with advanced colon cancer. *J Clin Oncol* 1994;12:1561–1571.
19. Willingham MC, Pastan I. Morphologic methods in the study of endocytosis in cultured cells. In: Pastan I, Willingham MC, eds. *Endocytosis.* New York: Plenum Press;1985;281–320.
20. Bagshawe KD, Sharma SK, Southall PJ, et al. Selective uptake of toxic nucleoside (^{125}IUdR) by resistant cancer. *Br J Radiol* 1991;64:37–44.
21. Mariani G, Cei A, Collecchi P, et al. Tumor targeting in vivo and metabolic fate of 5-[iodine-125]iodo-2′-deoxyuridine following intratumoral injection in patients with colorectal cancer. *J Nucl Med* 1993;34:1175–1183.
22. Daghighian F, Humm J, Macapinlac H, et al. Pharmacokinetics and dosimetry ^{125}I-IUdR in the treatment of colorectal cancer metastatic to liver. *J Nucl Med* 1996; 37:(suppl):29S–32S.
23. Macapinlac HA, Kemeny N, Daghighian F, et al. Pilot clinical trial of ^{125}I-5′-iododeoxyuridine in the treatment of colorectal cancer metastatic to the liver. *J Nucl Med* 1996;37:(suppl):25S–29S.
24. Kassis AI, Adelstein SJ, Haydock C, Sastry KSR. Radiotoxicity of ^{75}Se and ^{35}S: theory and application to a cellular model. *Radiat Res* 1980;84:407–425.
25. Lindmo T, Boven E, Mitchell JB, Morstyn G, Bunn PA. Specific killing of human melanoma cells by ^{125}I-labeled 9.2.27 monoclonal antibody. *Cancer Res* 1985;45: 5080–5087.
26. Woo DV, Li D, Mattis JA, Steplewski Z. Selective chromosomal damage and cytotoxicity of ^{125}I-labeled monoclonal antibody 17-1-A in human cancer cells. *Cancer Res* 1989;49:2952–2958.
27. Cole A. Absorption of 20-eV to 50,000-eV electron beams in air and plastic. *Radiat Res* 1969;38:7–33.